

Elsevier Editorial System(tm) for Precambrian Research

Manuscript Draft

Manuscript Number:

Title: Paleomagnetism and geochronology of the Malani Igneous Suite, Northwest India: Implications for the configuration of Rodinia and the assembly of Gondwana

Article Type: Research Paper

Section/Category:

Keywords: Rodinia; Malani Igneous Suite; Neoproterozoic; continental reconstruction; Northwest India

Corresponding Author: Miss Laura C Gregory, B.S.

Corresponding Author's Institution: University of Florida

First Author: Laura C Gregory, B.S.

Order of Authors: Laura C Gregory, B.S.; Joseph G Meert, PhD; Bernard Bingen, PhD; Manoj K Pandit, PhD; Trond H Torsvik, PhD

Manuscript Region of Origin:

Abstract: The configuration of the Precambrian supercontinent Rodinia and the subsequent assembly of Gondwana are under considerable debate due to a paucity of high quality paleomagnetic data. The Indian continent is crucial to this topic and plays an essential role in the history of East Gondwana amalgamation. In proto-Gondwana reconstructions the location of the central Indian craton is important in testing the existence and age of the proposed Rodinia supercontinent. Improved paleomagnetic and geochronologic data collected from numerous dikes in central India will help to better constrain the details of the supercontinent. We have collected samples from 4 late stage mafic dikes that intrude the Jalore Granite in the Malani Igneous Suite (MIS) in Rajasthan, Central India. The MIS is primarily composed of felsic rocks

that erupted in initial voluminous flows, which were shortly intruded by granitic plutons. The large (up to 5 m wide) mafic dikes mark the final phase of igneous activity and were the targets of our investigation. Previous age constraints from the Malani suite are either reported as personal communications or are unreliable Rb/Sr dates and do not provide a complete picture of the tectonic evolution of the continent during the Rodinia breakup. We obtained a paleomagnetic direction with declination=349.8° and inclination=64.1° ( $k=116.4$  and  $\alpha_{95}=11.5^\circ$ ), that overlaps with previously reported results. In addition, fine-grained mafic dikelets show reversed directions with a declination=195.3° and inclination=-59.7° ( $k=234.8$  and  $\alpha_{95}=8.1^\circ$ ) and also record an overprint of normal polarity from the larger dikes. We also report an U/Pb age of  $771 \pm 5$  Ma from zircons in the Malani rhyolitic tuff and we are currently in the process of calculating an  $^{40}\text{Ar}/^{39}\text{Ar}$  whole-rock age. These data combined with a baked contact test truly solidify the paleomagnetic pole, and thus give insight into the complicated Proterozoic and Early Cambrian history of India.

1 **Paleomagnetism and geochronology of the Malani Igneous Suite,**  
2 **Northwest India: Implications for the configuration of Rodinia and the**  
3 **assembly of Gondwana**

4 *Laura C. Gregory<sup>1,\*</sup>, Joseph G. Meert<sup>1</sup>, Bernard Bingen<sup>2</sup>, Manoj K. Pandit<sup>3</sup>,*  
5 *and Trond H. Torsvik<sup>2,4,5</sup>*

6  
7 <sup>1</sup>Department of Geological Sciences, University of Florida, 241 Williamson Hall,  
8 Gainesville, FL 32611

9 <sup>2</sup>Geological Survey of Norway, N-7491, Trondheim, Norway

10 <sup>3</sup>Department of Geology, University of Rajasthan, Jaipur, 302004, Rajasthan, India

11 <sup>4</sup>PGP, University of Oslo, 0316 Oslo (Norway)

12 <sup>5</sup>School of Geosciences, Private Bag 3, University of Witwatersrand, WITS2050, South  
13 Africa

14  
15  
16 \*Corresponding author: L.C. Gregory (lalaura@ufl.edu)  
17

18

19

20

21

22

23

24

25

26

27

28

29 **Abstract**

30         The configuration of the Precambrian supercontinent Rodinia and the subsequent  
31 assembly of Gondwana are under considerable debate due to a paucity of high quality  
32 paleomagnetic data. The Indian continent is crucial to this topic and plays an essential  
33 role in the history of East Gondwana amalgamation. In proto-Gondwana reconstructions  
34 the location of the central Indian craton is important in testing the existence and age of  
35 the proposed Rodinia supercontinent. Improved paleomagnetic and geochronologic data  
36 collected from numerous dikes in central India will help to better constrain the details of  
37 the supercontinent. We have collected samples from 4 late stage mafic dikes that intrude  
38 the Jalore Granite in the Malani Igneous Suite (MIS) in Rajasthan, Central India. The  
39 MIS is primarily composed of felsic rocks that erupted in initial voluminous flows, which  
40 were shortly intruded by granitic plutons. The large (up to 5 m wide) mafic dikes mark  
41 the final phase of igneous activity and were the targets of our investigation. Previous age  
42 constraints from the Malani suite are either reported as personal communications or are  
43 unreliable Rb/Sr dates and do not provide a complete picture of the tectonic evolution of  
44 the continent during the Rodinia breakup. We obtained a paleomagnetic direction with  
45 declination=349.8° and inclination=64.1° (k=116.4 and  $\alpha_{95}$ =11.5°), that overlaps with  
46 previously reported results. In addition, fine-grained mafic dikelets show reversed  
47 directions with a declination=195.3° and inclination=-59.7° (k=234.8 and  $\alpha_{95}$ =8.1°) and  
48 also record an overprint of normal polarity from the larger dikes. We also report an U/Pb  
49 age of 771 ±5 Ma from zircons in the Malani rhyolitic tuff and we are currently in the  
50 process of calculating an  $^{40}\text{Ar}/^{39}\text{Ar}$  whole-rock age. These data combined with a baked  
51 contact test truly solidify the paleomagnetic pole, and thus give insight into the  
52 complicated Proterozoic and Early Cambrian history of India.

53 Keywords: Rodinia, Malani Igneous Suite, Neoproterozoic, continental reconstruction,  
54 NW India  
55

56

57

58

59

60

61

62

63

64

65

66

67

68

69

70

71

72

73

74

75

76

77 **1. Introduction**

78         The notion of a Meso- to Neoproterozoic supercontinent that formed in the  
79 aftermath of the Grenvillian orogeny began to develop in the 1970's (Piper, 1976, Bond  
80 et al., 1984). The name of 'Rodinia' was proposed in the early 1990's (McMenamin and  
81 McMenamin, 1990; Dalziel, 1991; Moores, 1991; Hoffman, 1991; see also Meert and  
82 Torsvik, 2003). There are myriad models for the configuration of the Rodinia  
83 supercontinent and the exact locations of its constituent parts are unresolved. The  
84 archetypal model for Rodinia outlines that it began to form at about 1300 Ma and reached  
85 maximum size at about 1000 Ma. Fragmentation and breakup of Rodinia eventually was  
86 initiated along a rift between western (present-day coordinates) Laurentia and East  
87 Antarctica-Australia sometime between 800-700 Ma (Bond et al., 1984; Dalziel 1991;  
88 Hoffman, 1991; Powell et al., 1993). At that point, it is hypothesized that rifting heralded  
89 a period of intense global cooling, sparking the development of multi-cellular life on  
90 Earth (Hoffman, 1998, McMenamin and McMenamin, 1990, Meert, 2003; Meert and  
91 Liberman, 2008). Knowledge of the distribution and geotectonic evolution of continents  
92 during the Neoproterozoic is critical for an improved understanding of the context and  
93 causes of extreme climatic changes and accelerated biologic evolution at the boundary  
94 between the Neoproterozoic and the Paleozoic.

95         The fragmentation of Rodinia was followed by the assembly of the superterrane  
96 Gondwana. East Gondwana is composed of cratonic blocks of India, Madagascar, Sri  
97 Lanka, East Antarctica, Australia and the Seychelles. The paleogeography of the cratons  
98 that make up East Gondwana prior to the formation of and after severance from Rodinia  
99 is debated. Some (Windley et al., 1994; Piper, 2000; Yoshida and Upreti, 2006; Squire et

100 al., 2006; Paulsen et al., 2007) argue that these cratons came together in a single  
101 collisional event around or even earlier than 1300 Ma, and stayed in the same  
102 configuration within Rodinia and up to the formation of Gondwana. However, this  
103 scenario is viewed with skepticism. The alternative formation of Gondwana as a  
104 polyphase assembly of cratonic nuclei that had previously dispersed from the Rodinia  
105 supercontinent seems to be more consistent with available geologic, paleomagnetic and  
106 geochronologic data (Meert et al., 1995; Meert and Powell, 2001; Meert and Torsvik,  
107 2003; Boger et al., 2002; Fitzsimons, 2000; Pisarevsky et al., 2003; Collins and  
108 Pisarevsky, 2005, Meert and Liberman, 2008). This dispute may be resolved through the  
109 acquisition of high-quality paleomagnetic data coupled to high-resolution geochronologic  
110 ages from the various cratons that comprise Gondwana. Unfortunately, many studies are  
111 incomplete in that they do not incorporate an age with paleoposition and thus do not  
112 place strong spatial-temporal constraints on ancient continental localities (Meert and  
113 Powell, 2001).

114         The location of India within Gondwana is critical for evaluating the various  
115 tectonic models related both to the assembly of greater Gondwana and models of  
116 Rodinia. Greater India is placed alongside East Antarctica in the traditional Gondwana  
117 fit at 560 Ma (Figure 1, de Wit et al., 1988). A traditional Gondwana fit would situate  
118 India at low latitudes at 750 Ma in order to comply with the geometry of Rodinia prior to  
119 breakup and the determined fit for East Antarctica. Paleomagnetic data are in  
120 disagreement with a low-latitude location for India at 750 Ma, and instead, the extant data  
121 imply a significantly higher paleolatitude (Torsvik et al., 2001a,b).

122 The tectonic setting of India during the proposed interval of Rodinia breakup is  
123 also unclear, and pertinent to deciphering its ancient location. Bhushan (2000) implied  
124 that the predominantly felsic magmatism of the Malani Igneous Suite (MIS) in  
125 northwestern India is a result of thermal melting of the base of the crust in a rift setting at  
126 around 700 to 800 Ma. The MIS is often described as ‘anorogenic magmatism’ related  
127 either to crustal melting during extension or to an active hot spot (Bhushan, 2000;  
128 Sharma, 2004). Alternatively MIS magmatism can be interpreted in the context of an  
129 Andean-type active margin (Torsvik et al., 2001a; Torsvik et al., 2001b, Ashwal et al.,  
130 2002), closely related to the nearby arc activity observed in the Seychelles islands and  
131 northeastern Madagascar, which lay along NW India at about 750 Ma. Magmatic activity  
132 in the Seychelles and northeastern Madagascar is attributed to northeastward subduction  
133 of the Mozambique Ocean (Handke et al., 1999; Meert et al., 2003; Tucker et al., 1999).  
134 The duration of magmatism and the source of igneous activity in the area are still  
135 questionable. In this paper, we report paleomagnetic and geochronologic data for the  
136 Malani Igneous Suite (MIS) in Rajasthan, northwestern India, one of the largest (51,000  
137 km<sup>2</sup>) felsic igneous suites in the world (Pareek, 1981; Bhushan, 2000) of accepted  
138 Neoproterozoic age (Figure 2). Paleomagnetic data from late stage mafic dikes paired  
139 with a U-Pb study of a rhyolitic tuff provides an improved, demonstrably primary,  
140 paleomagnetic pole for the MIS with a reliable temporal constraint. The data are used to  
141 derive a key paleopole for the Indian plate during the Neoproterozoic, and lead to a  
142 discussion on the drift of India between the dispersal of Rodinia and the formation of  
143 Gondwana.

## 144 **2.Geology and Tectonic Setting**

145           Magmatism in the Malani Igneous Suite (MIS) occurred in three intrusion phases.  
146 Activity commenced with an initial volcanic phase made up of basaltic then felsic flows.  
147 The second phase is characterized by the intrusion of granitic plutons. Predominately  
148 felsic and minor mafic dike swarms form the third and final phase of the igneous cycle.  
149 Malani felsic rocks are unmetamorphosed, but slightly tilted and folded. Late stage mafic  
150 dikes are all vertical to sub-vertical (Figures 3 and 4). The MIS unconformably overlies  
151 Paleo- to Mesoproterozoic metasediments, and basement granite gneisses and  
152 granodiorites of an unknown age (Pandit et al., 1999); and is unconformably overlain by  
153 the latest Neoproterozoic to Cambrian Marwar Supergroup made up of red-bed and  
154 evaporite sedimentary sequences (Pandit et al., 2001; Torsvik et al., 2001a).

155           A volcanoclastic conglomerate lies at the base of MIS (Bhushan, 2000) and basal  
156 rhyolitic tuffs denote the initiation of basaltic and largely felsic flows of the first stage of  
157 the suite. This is followed by the emplacement of granitic plutons and felsic dikes.  
158 Vertical to sub-vertical dolerite dikes crosscut all of the other components and thus mark  
159 the termination of magmatism. These mafic dikes intrude the Jalore Granite plutons  
160 south of Jodhpur and can be wide, up to 5 meters in extent (Figures 2, 3, and 4). The  
161 mafic dike sequence near Jalore contains a relatively dense concentration of dikes with a  
162 general N-S trend. Many of the larger dikes form conspicuous ridges only when enclosed  
163 in a granite host (Figure 4). Fresh in-place outcrop is difficult to find but we sampled 4  
164 dikes within the sequence, most of which were N-S trending dikes, including a very thin  
165 N-S trending dikelet that is cut by a wider E-W trending dike. This dikelet is less than 2  
166 cm wide, extremely fine grained and dark grey-black in color with obvious chilled  
167 margins (Figure 3b).

168           Among the multitude of tectonic settings proposed for Malani magmatism, it has  
169 been suggested (see Bhushan, 2000) that the first stage of associated basaltic and felsic  
170 flows is generated by a hot spot source or lithospheric thinning and melting at the base of  
171 the crust. However, India magmatism can also be compared with other Neoproterozoic  
172 igneous provinces. Paleomagnetic data juxtapose India alongside the Seychelles, and  
173 northeastern Madagascar is also placed along the India margin based on temporal and  
174 geological similarities (Ashwal et al., 2002). Both Madagascar and Seychelles have  
175 igneous activity from this time that is attributed to subduction (Figure 5; Torsvik et al.,  
176 2001b, Tucker et al., 2001, Ashwal et al., 2002). The paleoposition of India (at the  
177 western margin of Rodinia) in relation to the ancient supercontinent Rodinia and proto-  
178 East Gondwana, based on previous studies, conflicts with the hypothesis of rift tectonics  
179 and is more indicative of an Andean-type arc environment resulting from the subduction  
180 of the eastern Mozambique Ocean (Meert and Torsvik, 2003).

### 181 **3. Previous Studies**

#### 182 *3.1 Paleomagnetism*

183           Numerous paleomagnetic studies have been performed on the felsic members of  
184 the MIS to determine the paleoposition of India (Table 1). Athavale et al. (1963) were  
185 the first to apply paleomagnetic tests to rhyolitic flows, and their results are similar to  
186 those obtained by Klootwijk (1975), but lack any detailed stability tests. Torsvik et al.  
187 (2001a) found a statistically positive fold test on felsic rocks from Malani. Folding of the  
188 Malani rocks is post-eruption and pre-Marwar age, which constrains the age of the  
189 Malani pole to older than Cambrian. No reversals or other field tests have been found to  
190 further document the exact age of the magnetism. The lack of available or positive field

191 tests to fully constrain the age of magnetic acquisition may lead to doubt regarding the  
192 primary nature of the Malani pole.

### 193 *3.2 Geochronology*

194 Previous geochronologic results from Malani felsic volcanics span about 100  
195 million years (Table 2). Crawford and Compston (1970) reported a pioneering Rb-Sr age  
196 of  $730 \pm 10$  Ma for rhyolites (recalculated with a decay constant of  $1.42 \times 10^{-11}$ ; see  
197 Steiger and Jager, 1977). Later, Dhar et al. (1996) and Rathore et al. (1999) reported  
198 whole-rock Rb-Sr isochron ages for felsic volcanic rocks and granite plutons, emplaced  
199 during the first two stages of activity in the MIS (first and second stages, respectively),  
200 ranging from  $779 \pm 10$  to  $681 \pm 20$  Ma. This wide distribution of dates is partially a result  
201 of studies of the so-called ultrapotassic rhyolites found near our sampling locality. The  
202 youngest age Rb-Sr isochron age of  $681 \pm 20$  Ma (Rathore et al., 1999) comes from a  
203 solitary occurrence of the “ultrapotassic” rhyolite (Figure 2), without any rock description  
204 that would ascertain whether high potassium is a primary igneous character or a later  
205 alteration effect. Much younger apparent ages of  $548 \pm 7$  to  $515 \pm 6$  Ma were obtained  
206 from whole-rock  $^{40}\text{Ar}/^{39}\text{Ar}$  data on Jalore granites. These apparent ages are interpreted as  
207 evidence for a thermal disturbance by Rathore et al. (1999), and are perhaps related to the  
208 Kuungan orogen (Meert 2003). Torsvik et al. (2001a) cited precise U-Pb ages of  $771 \pm 2$   
209 and  $751 \pm 3$  Ma for rhyolite magmatism in the MIS (Tucker et al., unpublished), but  
210 without analytical details and sample descriptions.

## 211 **4. Methods**

### 212 *4.1 Paleomagnetic Experiments*

213 Samples were obtained in the field using a gasoline powered hand drill and  
214 oriented using magnetic and sun compasses. Readings from the sun compass were used

215 to correct for the local declination and any magnetic interference from the outcrop.  
216 Twelve samples from Jalore Granite and about 50 samples from four mafic dikes were  
217 taken at three sites. Three of the granite samples include a very small (width less than 2  
218 cm) fined grained N-S trending dikelet, which is cut by the wide E-W trending mafic dike  
219 (Figure 3b).

220 Samples were cut into standard sized specimens and stored in a magnetically  
221 shielded space in the University of Florida paleomagnetic laboratory. A few preliminary  
222 samples were stepwise treated thermally or using an alternating field to determine the  
223 best method of demagnetization. After analyzing the behavior of preliminary samples, a  
224 series of steps were chosen for either alternating field or thermal demagnetization.  
225 Alternating field demagnetization was applied in a step-wise manner using a home-built  
226 AF-demagnetizer at fields up to 140 mT. Samples were also treated thermally in a  
227 stepwise manner, up to temperatures of 600°C for ~60 minutes using an ASC-Scientific  
228 oven. Between each treatment, strong samples, generally the mafic dikes, were measured  
229 on a Molspin Magnetometer and weaker samples, generally dikelets and granites, were  
230 measured on an ScT cryogenic magnetometer. Characteristic remanence components  
231 (ChRc) were calculated with the least-square regression analysis implemented in the  
232 Super IAPD program (<http://www.ngu.no/geophysics>; Kirschvink, 1980).

#### 233 *4.2 Rock Magnetic Experiments*

234 The magnetic susceptibility of each sample was measured on an Agico SI-3B  
235 bridge before treatment. Curie temperature experiments were run using a KLY-3S  
236 susceptibility bridge with a CS-3 heating unit. For this experiment, the susceptibility of a  
237 crushed sample is measured at increments during heating and cooling. The character of  
238 magnetic minerals in the sample can then be determined in detail based on the change in

239 susceptibility. Isothermal Remanence Acquisition (IRM) studies were also performed  
240 using an ASC-IM30 impulse magnetizer to further characterize magnetic mineralogy.

#### 241 *4.3 Geochronology*

242 Zircon was purified from one sample of rhyolitic tuff using a water table, heavy  
243 liquids and a magnetic separator. Available crystals were mounted in epoxy and polished  
244 to approximately half thickness. Cathodoluminescence (CL) images were obtained with  
245 a scanning electron microscope (Figure 6). U-Pb analyses were performed by secondary  
246 ion mass spectrometry (SIMS) using the CAMECA IMS 1270 instrument at the NORDSIM  
247 laboratory, Swedish Museum of Natural History, Stockholm (Table 3). The analytical  
248 method, data reduction, error propagation and assessment of the results are outlined in  
249 Whitehouse et al. (1999). The analyses were conducted with a spot size of ca. 20  $\mu\text{m}$ ,  
250 calibrating to the Geostandard of 91500 reference zircon with an age of 1065 Ma  
251 (Wiedenbeck et al., 1995). The error on the U-Pb ratio includes propagation of the error  
252 on the day-to-day calibration curve obtained by regular analysis of the reference zircon.  
253 A common Pb correction was applied using the  $^{204}\text{Pb}$  concentration and present-day  
254 isotopic composition (Stacey and Kramers, 1975). The ISOPLOT program (Ludwig, 1995)  
255 was used to regress and present the SIMS U-Pb data.

### 256 **5. Results**

#### 257 *5.1 Geochronologic Results:*

258 Zircon U-Pb geochronology was conducted on a sample of unfoliated rhyolitic  
259 tuff representing the first stage of volcanism in the MIS. The sample, Mis5/04, was  
260 collected close to Jodhpur (26°17.963'-72°58.357') at site 3 of Torsvik et al. (2001a).  
261 The sample shows ca. 5mm automorphic phenocrysts of quartz, plagioclase and K-  
262 feldspar in a microcrystalline devitrified groundmass of rose color. The sample contains

263 few large (ca. 200  $\mu\text{m}$ ) prismatic zircon crystals. They show well-terminated pyramid tips  
264 and oscillatory zoning. They contain common fluid and mineral inclusions. Their habit  
265 is typical for zircon formed in a volcanic/subvolcanic magmatic environment. Sixteen  
266 analyses were made on 10 zircon crystals. Fourteen of them are concordant and define a  
267 concordia age of  $771 \pm 5$  Ma (MSWD = 1.5; Figure 6). This age is interpreted as the  
268 timing of magmatic crystallization and deposition of the rhyolite tuff.

### 269 *5.2 Rock Magnetic Results:*

270 Curie temperature runs on the mafic dike samples show a curve that is  
271 characteristic of magnetite, but with some alteration upon cooling (Figure 7b).  
272 Susceptibility is higher on heating than cooling, but curie temperatures are similar and in  
273 the typical range of magnetite. The heating Curie temperature  $T_{cH}$  is equal to  $589.7^\circ\text{C}$   
274 and the cooling Curie temperature  $T_{cC}$  is equal to  $588.3^\circ\text{C}$ . Curie temperature tests for  
275 dikelet samples show a low susceptibility heating curve that may be a result of  
276 titanomagnetite and a cooling curve with higher susceptibility resulting from exsolution  
277 of titanomagnetite to form pure magnetite (Figure 7c). Mafic dikes also have an  
278 Isothermal Remanance Magnetization (IRM) plot that is indicative of magnetite (Figure  
279 7a). Samples saturate at  $\sim 0.3$  tesla and their intensity remains constant at higher fields,  
280 up to the highest applied field of 2 tesla. Sample I434-28 is a mafic dikelet, and has an  
281 IRM curve also characteristic of magnetite, but with a lower absolute J value at  
282 saturation. Thermal demagnetization curves show unblocking at the characteristic  
283 magnetite temperature range of  $550$  to  $570^\circ\text{C}$  (Figure 8a).

### 284 *5.3 Paleomagnetic Results*

285 Table 4 lists paleomagnetic results from each site in this study. Figure 8 shows  
286 the typical demagnetization plots of two mafic dike sites. Most samples show a stable

287 demagnetization trend, dependent on the treatment applied. Thermally treated samples  
288 unblock between 550 and 570° C and quickly lose over 50 percent of their intensity at  
289 this temperature range (Figure 8a). Samples treated with an alternating field lose  
290 intensity at a more gradual rate and do not generally unblock past greater than 80-85  
291 percent of the original strength (Figure 8b). Most samples have a low temperature or low  
292 coercivity overprint that has no consistent direction, but is quickly removed. Jalore  
293 granite samples were taken with the intent to perform a baked contact test, but samples  
294 are dominated by multi-domain grains that have a strong, but unstable remanence (even  
295 with the application of low-temperature demagnetization).

296 Three samples were taken from the less than 2 cm wide dikelet pictured in figure  
297 2b. The larger dike at site 34 crosscuts this very fine grained dike. When treated with  
298 both alternating field and thermal demagnetization, samples display oppositely directed  
299 magnetization from the three larger Malani dikes (Figure 10). Demagnetization trends  
300 include two distinct components and are weaker in intensity than those from the larger  
301 dikes. They show an increase in intensity at temperatures up to about 490°C or fields to  
302 40 mT. The low temperature and coercivity component is identical to the mean direction  
303 from the normal polarity dikes and we interpret this as evidence of baking of the smaller  
304 dike by the larger E-W trending dike. The baked overprint component has a  
305 declination=2.5, inclination=+57.5 (with  $k=17.1$  and  $\alpha_{95}=30.8$ ). The high temperature  
306 and coercivity component has a reverse polarity with declination=195.3° and  
307 inclination=-59.7° (with  $k=234.8$  and  $\alpha_{95}=8.1$ ). The McFadden and McElhinny (1990)  
308 reversal test demonstrates an angle of 10° between the three normal site means and the

309 reverse polarity individual samples. Although only a VGP, the reversal test has a  
310 classification of C.

311 The mean direction from all sites has a declination=349.8° and inclination=64.1°  
312 (with  $k=116.4$  and  $\alpha_{95}=11.5$ ). Site I434 demonstrated reverse polarity in three samples of  
313 a small fine-grained dike. After inverting the reverse polarity direction, the mean  
314 direction from all four dikes has declination=358.8° and inclination=63.5° (with  $k=91.2$   
315 and  $\alpha_{95}=9.7$ ; Figure 9). The paleomagnetic pole calculated from the mean direction from  
316 each site falls at 68.5°N, 58.1°E ( $dp=14.8^\circ$ ,  $dm=18.5^\circ$ ). The mean paleomagnetic pole  
317 calculated from an average VGP of each site is 68.6°N, 57.5°E ( $A95=13.4^\circ$ ).

## 318 **6. Discussion**

### 319 *6.1 Significance of paleomagnetic and geochronologic data*

320 When results from Malani mafic dikes (this study) and rhyolitic volcanics  
321 (Torsvik et al., 2001a) are combined, a grand mean paleomagnetic pole for the MIS can  
322 be placed at 69.0°N, 83.2°E ( $dp=8.8^\circ$ ,  $dm=10.9^\circ$ ), which translates into a paleolatitude of  
323 46.5° (+9.6°, -8.0°) for the Malani igneous suite at Jalore. The Malani pole has been  
324 cited as the representative pole for India during the late Neoproterozoic, yet the lack of a  
325 conclusive reversal or a field test was used by some authors to conclude that the  
326 paleomagnetic data were untrustworthy (see Yoshida and Upreti, 2006 for example).  
327 However the results of our study provide additional evidence for a primary  
328 magnetization. The fold test provided by Torsvik et al. (2001a) is now augmented by a  
329 baked contact test and dual polarity. The baked contact test lies in the normal polarity  
330 overprint that is found in fine-grained dikelet samples. This is a distinct overprint at low  
331 temperature and coercivity demagnetization acquired from crosscutting, normal polarity  
332 dikes. The anti-podal direction is close to 180° different from the reversed signature of

333 the smaller dikes (Figure 10). In addition, the Malani pole does not overlap with any  
334 recent poles from the Indian subcontinent. The Malani pole has a unique location when  
335 compared to common overprints in India (Deccan and Rajmahal Traps), which further  
336 attests the quality of this pole (Figure 9).

337 No reverse polarity direction was noted in previous studies of the MIS. Torsvik et  
338 al., (2001a) did resolve a B component in their samples that trends towards a reverse  
339 polarity direction, but it was not antipodal to the normal polarity component. They  
340 attributed it to a secondary origin, possibly due to hydrothermal alteration. In our study,  
341 all samples taken from the small fine-grained mafic dikelet demonstrate a reverse polarity  
342 direction, with a normal polarity overprint. The vector was not found in large dikes at the  
343 same site. The reverse direction is exactly antipodal and passes the McFadden and  
344 McElhinny reversal test with a C, which is significant when considering the unfortunately  
345 small sampling section that was available for the reversed polarity rocks. Although only  
346 a VGP, this reversed direction further validates the primary nature of the pole. We stress  
347 that our VGP combined with previous study (Torsvik et al., 2001a) provides the most  
348 reliable and precise Neoproterozoic pole for India.

349 The new zircon extrusion age of  $771 \pm 5$  Ma (Fig. 6) for a rhyolitic tuff places a  
350 robust pin on the timing of the first stage of magmatism in the MIS. This age is  
351 consistent with the oldest available Rb-Sr isochron age of  $779 \pm 10$  Ma (Rathore et al.,  
352 1999), based on felsic volcanic rocks from widely spaced sampling sites. It is also  
353 consistent with the first of two unpublished zircon dates at  $771 \pm 2$  and  $751 \pm 3$  Ma quoted  
354 by Torsvik et al. (2001a) for rhyolite magmatism in the first stage of MIS magmatism.  
355 Available Rb-Sr whole-rock geochronology (Crawford and Compston, 1970; Dhar et al.,

356 1996; Rathore et al., 1999) defines a time span of nearly 100 m.y. ( $779 \pm 10$  to  $681 \pm 20$   
357 Ma), so one cannot rule out that the second and third stages of the magmatism are  
358 significantly younger than  $771 \pm 5$  Ma. Nevertheless, the consistency of paleomagnetic  
359 data for the different stages of magmatism argues for a comparatively short duration of  
360 magmatism. In Figure 11, published paleopoles determined from the early stage of  
361 rhyolitic magmatism in the MIS (Athavale, 1963; Klootwijk, 1975; Torsvik et al., 2001a)  
362 are compared to the paleopole derived from the third stage of magmatism of the suite  
363 (mafic dikes, this study). All studies show equivalent results (Figure 11). Thus India did  
364 not likely undergo a large extent of latitudinal movement during Malani magmatism,  
365 even with errors taken into account. With reference to paleomagnetic data, the duration  
366 of the Malani magmatism occurred without much change in location relative to the  
367 earth's spin axis. The eruption may not have occurred over a 100 million year span as  
368 suggested by Rb-Sr data (Rathore et al., 1999) because the Indian continent would likely  
369 have undergone recognizable latitudinal movement the prolonged magmatic activity.

370 The MIS is often stated to be the result of a rift setting or a mantle plume (Singh  
371 et al., 2006; Bhushan, 2000), despite the lack of large volumes of basaltic rocks that are  
372 generally the result of a large-scale mantle heating event. Malani rocks are also  
373 commonly attributed to Anorogenic-type (A-type) volcanism, but the mechanism for this  
374 eruption type has not been explicitly stated. Subduction of an ancient ocean, the  
375 Mozambique, has been suggested as a source for activity, but this has also been disputed  
376 because of the lack of deformation in the area. However, it is certainly possible that the  
377 undeformed Malani magmatic rocks represent the inboard result of a subduction zone,  
378 and that deformed margin material has been eroded or buried. Madagascar is commonly

379 placed alongside India in Gondwana-fit reconstructions, and Seychelles has been  
380 paleomagnetically placed adjacent to India's margin (Figure 5, Torsvik et al., 2001b).  
381 Both micro-continents have volcanism attributed to the subduction of a Neoproterozoic  
382 ocean (Torsvik et al., 2001b, Tucker et al., 2001, Ashwal et al., 2002). Considering the  
383 nature and timing of magmatism in the Seychelles and India, it appears that the bulk of  
384 granitic and subsequent mafic magmatism in those regions was constrained to the interval  
385 from ~771-751 Ma.

## 386 *6.2 Implications for the configuration of Rodinia*

387 It is suggested (Powell et al., 1993; Windley et al., 1994; Dalziel, 1997; Yoshida  
388 and Upreti, 2006) that a coherent East Gondwana existed from the Mesoproterozoic  
389 through the bulk of the Precambrian and until the assembly of Gondwana at 550-530 Ma.  
390 However this is largely based on data with high flexibility of interpretation and poor age  
391 control, as well as the lack of evidence for appropriately aged oceanic sutures between  
392 East Gondwana cratons. Yoshida and Upreti (2006) discuss evidence for the  
393 Neoproterozoic juxtaposition of India and Australia-East Antarctica based on similarities  
394 in cratonic and orogenic detrital zircon and neodymium isotopic signatures. Yet the  
395 notion of a united East Gondwana through the Proterozoic and Cambrian is contradicted  
396 by high quality paleomagnetic data (Meert and Van der Voo, 1997; Meert, 2001; Torsvik  
397 et al., 2001a), and also in Fitzsimons (2000) review of evidence for appropriately aged  
398 mobile belts separating distinct segments of East Gondwana elements, which accounts for  
399 a later (Cambrian) ocean closure. In their discussion of the proximity of India and  
400 Australia-East Antarctica, Yoshida and Upreti (2006) argue that the paleomagnetic data  
401 used to constrain the possible separation of these continents do not include a well-  
402 constrained age and have been reset by the later Pan-African event (~530-510 Ma). We

403 emphasize that this is not a valid argument because both the Malani pole reported in this  
404 paper and the highly reliable pole from the Mundine Well dike swarm in Australia  
405 (Wingate and Giddings, 2000) include necessary field and contact tests to argue against  
406 any resetting, and both are well-dated.

407         The paleolatitude of the Mundine Well dikes is  $20.2^{\circ}$  ( $+5.5^{\circ}$ ,  $-4.8^{\circ}$ ) and this can  
408 be compared to the paleolatitude of the Malani dikes from our study ( $46.5^{\circ}$ ,  $+9.6^{\circ}$ ,  $-8.0^{\circ}$ ),  
409 indicating a separation of greater than  $40^{\circ}$  in latitude using the conventional East  
410 Gondwana fit (Figure 12). For East Gondwana to be a coherent group at 750 Ma, it is  
411 necessary for India to be located along the paleoequator, according to its placement in the  
412 typically accepted Gondwana fit (deWit et al., 1988) relative to the locations of Australia  
413 and Antarctica within Rodinia reconstructions (Figure 12). It is possible that the  
414 southeast margin of India was located along the northwestern margin of Australia, but no  
415 geologic evidence such as oceanic sutures or similar-aged orogenic belts have been found  
416 to support this orientation. Younger-aged sutures between Gondwana components also  
417 indicate a more complex Gondwana amalgamation. The East Africa Orogen is described  
418 by Stern (1994) as an 800-650 Ma collision of IMSLEK cratons (*India, Madagascar, Sri*  
419 *Lanka, East Antarctica, and the Kalahari craton*) with the Congo craton and Arabian-  
420 Nubian shield (ANS). The later Kuunga Orogen (Meert et al., 1995) places the final  
421 Gondwana assembly at about 550 Ma with the amalgamation of Australia-Antarctica  
422 with the IMSLEK-Cong-ANS group. These major Pan-African orogenies are congruent  
423 with a younger East Gondwana assembly, and placing India alongside East Antarctica  
424 and Australia at 770 Ma fails to account for the existence of the considerably younger  
425 sutures.

426 *7. Conclusions*

427           The MIS provides the best paleomagnetic pole for the Indian subcontinent at  
428 ~750-770 Ma, with a combined pole that plots at 69.0° N, 83.2° E (dp=8.8°, dm=10.9°).  
429 Our study further strengthens the case for a primary magnetization from the MIS with a  
430 reversal found in mafic dikelets and a baked contact test. The first documented U-Pb age  
431 of 771±5 Ma provides a more accurate and concordant lower age limit for Malani  
432 volcanism. When combined with geochronologic data from mafic dykes in the  
433 Seychelles, our age determination also hints at a shorter duration of magmatic activity in  
434 the MIS than previously stated.

435           India was previously stated to be a part of East Gondwana from about 1.1 Ga until  
436 the assembly of Gondwana around 550 Ma (Yoshida and Upreti, 2006). However,  
437 paleomagnetic data place India and the Seychelles at higher latitudes than coeval poles  
438 from Australia (Wingate and Giddings, 2000). These three robust paleomagnetic results  
439 (Mundine dykes, Malani Igneous Suite and Mahe Dikes) argue strongly against an  
440 amalgamated East Gondwana at 750 Ma and explain the younger Pan-African belts  
441 between these cratons. Thus, we argue that if paleomagnetism is to make any  
442 contribution to Neoproterozoic plate tectonic models, the new Malani pole must be  
443 seriously considered in any geodynamic explanation for the assembly of Gondwana.

444

445 Acknowledgements: This work was supported by a grant (to JGM) from the National  
446 Science Foundation (EAR04-09101).

447

448

449

450 **References**

- 451 Ashwal, L.D., Demaiffe, D., Torsvik, T.H., 2002. Petrogenesis of neoproterozoic  
452 granitoids and related rocks from the Seychelles: evidence for the case of an  
453 Andean-type arc origin. *J. Petrology* 43, 45-83.
- 454 Athavale, R.N., Radhakrishnamurthy, C., Sahasrabudhe, P.W., 1963. Paleomagnetism of  
455 some Indian rocks, *Geophys. J. Roy. Astr. Soc.*, 7, 304-311.
- 456 Boger, S.D., Carson, C.J., Fanning, C.M., Hergt, J.M., Wilson, C.J.L., Woodhead, J.D.,  
457 2002. Pan-African intraplate deformation in the northern Prince Charles  
458 Mountains, east Antarctica. *Earth Planet Sci. Lett.* 195, 195-210.
- 459 Bond, G.C., Nickeson, P.A., Kominz, M.A., 1984. Breakup of a supercontinent between  
460 625 and 555 Ma: new evidence and implications for continental histories. *Earth*  
461 *Planet. Sci. Lett.* 70, 325-345.
- 462 Bhushan, S.K., 2000. Malani Rhyolites- A Review. *Gondwana Res.* 3, 65-77.
- 463 Collins, A.S., Pisarevsky, S.A., 2005. Amalgamating eastern Gondwana: The evolution  
464 of the Circum-Indian Orogens. *Earth Sci. Rev.* 71, 229-270.
- 465 Crawford, A.R., Compston, W., 1970. The age of the Vindhyan system of peninsular  
466 India. *Quart. J. Geol. Soc. Lond.* 125, 351-372.
- 467 Dalziel, I.W.D., 1991. Pacific margins of Laurentia and East Antarctica as a conjugate  
468 rift pair: evidence and implications for an Eocambrian supercontinent. *Geology*  
469 19, 598-601.
- 470 Dalziel, I.W.D., 1997. Neoproterozoic-Paleozoic geography and tectonics: Review,  
471 hypothesis and environmental speculation. *Bull. Geo. Soc. Am.* 109, 16-42.
- 472 DeWit, M.J., Jeffrey, M., Bergh, H. and Nicolaysen, L., 1988. Geologic map of sectors  
473 of Gondwana reconstructed to their disposition at 150 Ma (1:10,000,000). *Am.*  
474 *Assoc. Pet. Geol.*, Tulsa, Ok.
- 475 Dhar, S., Frei, R., Kramers, J.D., Nägler, T.F., Kochhar, N., 1996. Sr, Pb and Nd isotope  
476 studies and their bearing on the petrogenesis of the Jalore and Siwana complexes,  
477 Rajasthan, India. *J. Geo. Soc. India* 48, 151-160.
- 478 Fitzsimons, I.C.W., 2000. A review of tectonic events in the East Antarctic Shield and  
479 their implications for Gondwana and earlier supercontinents. *J. African Earth Sci.*  
480 31, 3-23
- 481 Handke, M.J., Tucker, R.D., Ashwal, L.D., 1999. Neoproterozoic continental arc  
482 magmatism in west-central Madagascar. *Geology* 27, 351-354.
- 483 Hoffman, P.F., Kaufman, A.J., Galen, P.H., Schrag, D.P., 1998. A Neoproterozoic  
484 Snowball Earth. *Science, New Series* 281, 1342-1346.
- 485 Hoffman, P.F., 1991. Did the breakout of Laurentia turn Gondwanaland inside out?  
486 *Science* 252, 1409-1412.
- 487 Kirschvink, J.L., 1980. The least-squares line and plane and the analysis of  
488 palaeomagnetic data. *Geophys. J. R. Astron. Soc.* 62, 699-718.
- 489 Klootwijk, C.T., 1975. A Note on the Palaeomagnetism of the Late Precambrian Malani  
490 Rhyolites near Jodhpur- India. *J. Geophys.* 41, 189-200.
- 491 Ludwig, K.R. (1995) Isoplot, version 2.82: a plotting and regression program for  
492 Radiogenic isotope data. 45 p. U.S. Geological Survey, Open-file report 91-445.
- 493 McFadden, P., McElhinny, M.W., 1990. Classification of the reversal test in  
494 paleomagnetism. *Geophys. J. Int.* 103, 725-729.
- 495 McMenamin, M.A.S., McMenamin, D.L.S., 1990. The Emergence of Animals; The

496 Cambrian Breakthrough. Columbia Univ. Press, New York. 217 pp.

497 Meert, J.G., Van der Voo, R., Ayub, S., 1995. Paleomagnetic investigation of the Gagwe  
498 lavas and Mbozi Complex, Tanzania and the assembly of Gondwana.  
499 Precambrian Res. 74, 225-244.

500 Meert, J.G., Van der Voo, R., 1997. The assembly of Gondwana 800-550 Ma. J.  
501 Geodyn. 23, 223-235.

502 Meert, J.G., 2001. Growing Gondwana and rethinking Rodinia. Gondwana Res. 4, 279  
503 288.

504 Meert, J.G., 2003. A synopsis of events related to the assembly of eastern Gondwana.  
505 Tectonophysics 362, 1-40.

506 Meert, J.G., Powell, C. McA., 2001. Introduction to the special volume on the assembly  
507 And breakup of Rodinia. Precambrian Res. 110, 1-8.

508 Meert, J.G., Torsvik, T.H., 2003. The making and unmaking of a supercontinent:  
509 Rodinia revisited. Tectonophysics 375, 261-288.

510 Meert, J.G., Nédélec, A., Hall, C., 2003. The stratoid granites of central Madagascar:  
511 paleomagnetism and further age constraints on neoproterozoic deformation.  
512 Precamb. Res. 120, 101-129.

513 Meert, J.G. and Lieberman, B.S., 2008. The Neoproterozoic assembly of Gondwana and  
514 its relationship to the Ediacaran-Cambrian radiation, Gondwana Res.,  
515 doi:10.1016/j.gr2007.06.007.

516 Moores, E.M., 1991. Southwest U.S.-East Antarctica (SWEAT) connection: a  
517 hypothesis. Geology 19, 425-428.

518 Pandit, M.K., Shekhawat, L.S., Ferreira, V.P., Sial, A.N., Bohra, S.K., 1999.  
519 Trondhjemite and Granodiorite Assemblages from West of Barmer: Probable  
520 Basement for Malani Magmatism in Western India. J. Geo. Soc. of India 53, 89-  
521 96.

522 Pandit, M.K., Sial, A.N., Jamrani, S.S., Ferreira, V.P., 2001. Carbon isotopic profiles  
523 across the Bilara Group rocks of trans-Aravalli Marwar Supergroup in western  
524 India: Implications for Neoproterozoic – Cambrian transition. Gondwana Res. 4,  
525 387-394.

526 Pareek, H.S., 1981. Petrochemistry and petrogenesis of the Malani igneous suite, India:  
527 summary. Geol. Soc. Am. Bull. 1 (92), 67-70.

528 Paulsen, T.S., Encarnación, J., Grunow, A.M., Watkeys, M., 2007. New age constraints  
529 for a short pulse in Ross orogen deformation triggered by East-West Gondwana  
530 suturing, Gondwana Res., doi: 10.1016/j.gr.2007.05.011.

531 Powell, C.McA., McElhinny, M.W., Meert, J.G., Park, J.K., 1993. Paleomagnetic  
532 constraints on timing of the Neoproterozoic breakup of Rodinia and the Cambrian  
533 formation of Gondwana. Geology 21, 889-892.

534 Piper, J.D.A., 1976. Palaeomagnetic evidence for a Proterozoic supercontinent. Philos.  
535 Trans. R. Soc. Lond. A280, 469-490.

536 Piper, J.D.A., 2000. The Neoproterozoic Supercontinent: Rodinia or Palaeopangaea?  
537 Earth and Plan. Sci. Let. 176, 131-146.

538 Pisarevsky, S.A., Wingate, T.D., Powell, C.McA., Johnson, S., Evans, D.A.D., 2003.  
539 Models of Rodinia assembly and fragmentation, in Yoshida, M., Windley, B.F.,  
540 Dasgupta, S. (eds) 2003. *Proterozoic East Gondwana: Supercontinent Assembly  
541 and Breakup*. Geological Society, London, Special Publications, 206, 35-55.

542 Rathore, S.S., Venkatesan, T.R., Srivastava, R.K., 1999. Rb-Sr Isotope Dating of  
543 Neoproterozoic (Malani Group) Magmatism from Southwest Rajasthan, India:  
544 Evidence of Younger Pan African Thermal Event by  $^{40}\text{Ar}$ - $^{39}\text{Ar}$  Studies.  
545 Gondwana Res. 2, 271-281.

546 Sharma, K.K., 2004. The Neoproterozoic Malani magmatism of the northwestern Indian  
547 shield: Implications for crust-building processes. Proc. Indian Acad. Sci (Earth  
548 Planet Sci.) 113, 795-807.

549 Singh, A.K., Singh, R.K.B., Vallinayagam, G., 2006. Anorogenic Acid Volcanic rocks in  
550 the Kundal area of the Malani Igneous Suite, Northwestern India: geochemical  
551 and petrogenetic studies. J. Asian Earth Sci. 27, 544-557.

552 Stacey, J.S., and Kramers, J.D., 1975. Approximation of terrestrial lead isotope evolution  
553 by a two-stage model. Earth and Planetary Science Letters 26, 207–221.

554 Steiger, R.N. and Jager, E., 1977. Subcommittee on Geochronology: convention on the  
555 use of decay constants in geo- and cosmochronology, Earth Planet. Sci. Lett., 36,  
556 359-362.

557 Stern, R.J., 1994. Arc assembly and continental collision in the Neoproterozoic East  
558 African orogen: implications for the consolidation of Gondwanaland. Annu. Rev.  
559 Earth Planet. Sci. 22, 225-244.

560 Torsvik, T.H., Carter, L.M., Ashwal, L.D., Bhushan, S.K., Pandit, M.K., Jamtveit, B.,  
561 2001a. Rodinia refined or obscured: palaeomagnetism of the Malani igneous  
562 suite (NW India). Precambrian Res. 108, 319-333.

563 Torsvik T.H., Ashwal, L.D., Tucker, R.D., Eide, E.A., 2001b. Neoproterozoic  
564 geochronology and palaeogeography of the Seychelles microcontinent: the India  
565 link. Precambrian Res. 110, 47-59.

566 Tucker, R.D., Ashwal, L.D., Hamilton, M.A., Torsvik, T.H., Carter, L.M., 1999.  
567 Neoproterozoic silicic magmatism in northern Madagascar, Seychelles and NW  
568 India: clues to neoproterozoic supercontinent formation and dispersal. Geol. Soc.  
569 Am. Abst. Prog. 31, A317 (abstract).

570 Tucker, R.D., Ashwal, L.D., Torsvik, T.H., 2001. U-Pb geochronology of Seychelles  
571 granitoids: a Neoproterozoic continental arc fragment. Earth and Planetary Sci.  
572 Lett. 187, 27-38.

573 Whitehouse, M.J., Kamber, B.S., and Moorbath, S., 1999. Age significance of U–Th–Pb  
574 zircon data from early Archaean rocks of west Greenland – a reassessment based  
575 on combined ion-microprobe and imaging studies. Chemical Geology 160, 201-  
576 224.

577 Wiedenbeck, M., Allé, P., Corfu, F., Griffin, W.L., Meier, M., Oberli, F., Von Quadt, A.,  
578 Roddick, J.C., and Spiegel, W., 1995. Three natural zircon standards for U-Th  
579 Pb, Lu-Hf, trace element and REE analyses. Geostandards Newsletter 19, 1–23.

580 Windley, B.F., Razafiniparany, A., Razakamanana, T., Ackermund, D., 1994. Tectonic  
581 framework of the Precambrian of Madagascar and its Gondwana connections: a  
582 review and reappraisal. Geol. Rundsch. 83, 642-659.

583 Wingate, M.T.D., Giddings, J.W., 2000. Age and palaeomagnetism of the Mundine Well  
584 dyke swarm, Western Australia: implications for an Australia-Laurentia  
585 connection at 550 Ma. Precambrian Res. 100, 335-357.

586  
587

588 Yoshida, M., Upreti, B.N., 2006. Neoproterozoic India within East Gondwana:  
589 Constraints from recent geochronologic data from Himalaya. *Gond. Res.* 10, 349-  
590 356.  
591

592

593

594

595

596

597

598

599

600

601

602

603

604

605

606

607

608

609

610

611

612

613

614

615

616

617

618

619

620 **Figure Legends**

621

622 Figure 1: Typically accepted Gondwana fit for 560 Ma, taken from deWit et al., 1988.  
623 Reconstructions that use a Gondwana fit come from this model.

624

625 Figure 2: Map showing Precambrian stratigraphic units of the Aravalli Mountain Region  
626 in NW India with sampling area boxed (adapted from GSI publications and other  
627 published work).

628

629 Figure 3: (a) Photo of a large E-W trending dike at site I434 (b) Photo of 1 cm wide N-S  
630 trending mafic dikelet from site I434.

631

632 Figure 4: Satellite photo from Google Earth® of the mafic dikes in the Malani Igneous  
633 Suite near the city of Jalore. Large dikes trend N-S.

634

635 Figure 5: Reconstruction of India, Seychelles (Sey) and Madagascar (Mad) in India  
636 coordinates. Seychelles is placed according to the Euler pole defined in Torsvik et al.,  
637 (2001) and Madagascar is placed according to its Gondwana fit alongside India.

638

639 Figure 6: Inverse concordia diagram showing U-Pb analyses of zircon and CL image of  
640 one zircon crystal from a rhyolitic tuff representing the first stage of magmatism in the  
641 Malani Igneous Suite. The concordia age of  $771 \pm 5$  Ma reflects magmatic crystallization  
642 of the rock.

643

644 Figure 7: (a) Isothermal Remanence Magnetization (IRM) plots from four Malani  
645 samples. Sample I434-28 is a mafic dikelet. All samples saturate at about 0.3 tesla.  
646 (b) Curie temperature test of typical mafic dike sample from site I434. TcH indicates  
647 Curie temperature during heating, and TcC indicates Curie temperature during cooling,  
648 (c) Curie temperature test of a mafic dikelet. Due to alteration during heating,  
649 susceptibility of sample during cooling is much higher than during heating, and axes are  
650 labeled accordingly.

651

652 Figure 8: (a) Thermal and (b) alternating field (AF) demagnetization results of mafic  
653 samples from sites 35 and 36. In stereoplots, closed circles represent positive  
654 inclinations. In Zijderveld diagrams closed (open) circles represent the horizontal  
655 (vertical) plane. NRM= Natural Remanent Magnetization. Thermal measurements are in  
656 °C and AF measurements are in millitesla (mT).

657

658 Figure 9: Stereoplot of individual site means, overall mean and reversed polarity mean  
659 with common India overprints from the Deccan Traps and Rajmahal Traps indicated.

660

661 Figure 10: Demagnetization results from site 34. (a) Normal polarity sample subjected to  
662 AF demagnetization. (b) Reversed polarity dikelet sample with arrows pointing in  
663 direction from NRM to origin of both the overprint and reverse polarity vector. In  
664 stereoplots, closed circles represent positive inclinations. In Zijderveld diagrams closed  
665 (open) circles represent the horizontal (vertical) plane. NRM= Natural Remanent

666 Magnetization. Thermal measurements are in °C and AF measurements are in millitesla  
667 (mT).

668

669 Figure 11: Stereoplot of means from this study and previous studies from the Malani  
670 Igneous Suite, with our reverse polarity mean and the C component from Torsvik et al.,  
671 (2001a) indicated. Closed circles represent positive inclinations.

672

673 Figure 12: Reconstruction at 770 Ma of pertinent East Gondwana components. Grey  
674 India outline is plotted as a VGP from this study, with the Seychelles euler rotation fit  
675 from Torsvik et al., (2001b) and Madagascar is placed according to the Gondwana fit.  
676 Australia is plotted according to the Mundine Wells dikes VGP, and Antarctica and India  
677 are placed in their Gondwana fit locations, in the Australia reference frame. There is  
678  $>20^\circ$  of latitudinal displacement between the Malani and Mundine Wells study sites.

Figure 1

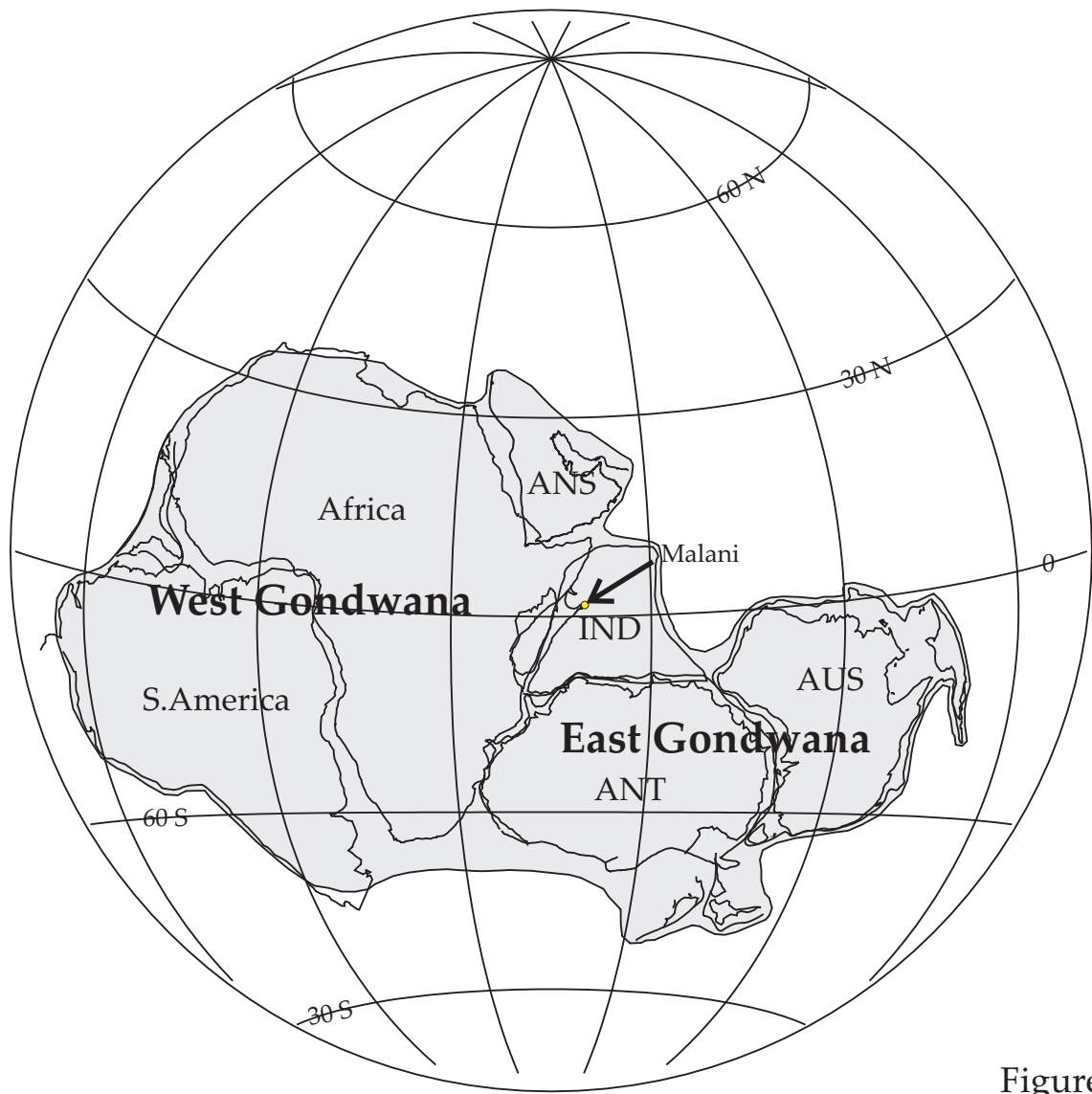


Figure 1

Figure 2

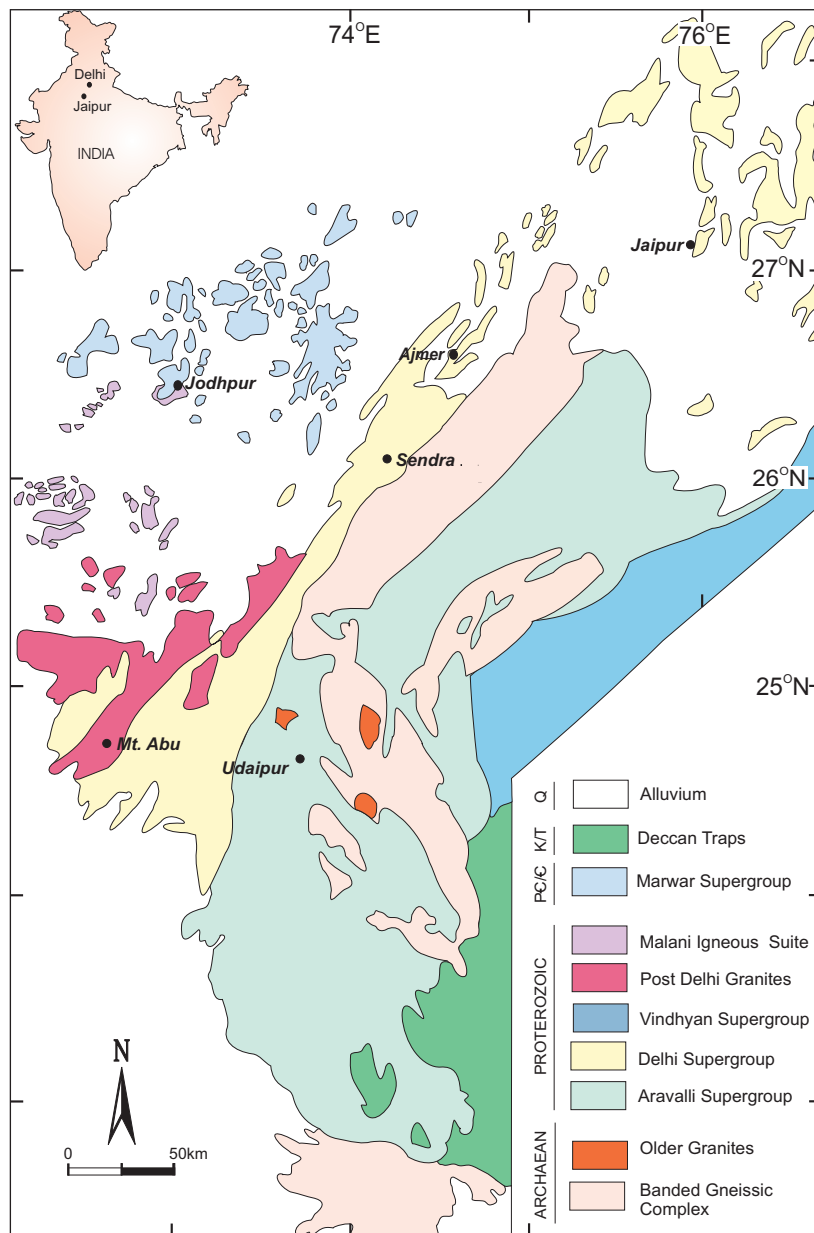


Figure 2

Figure 3

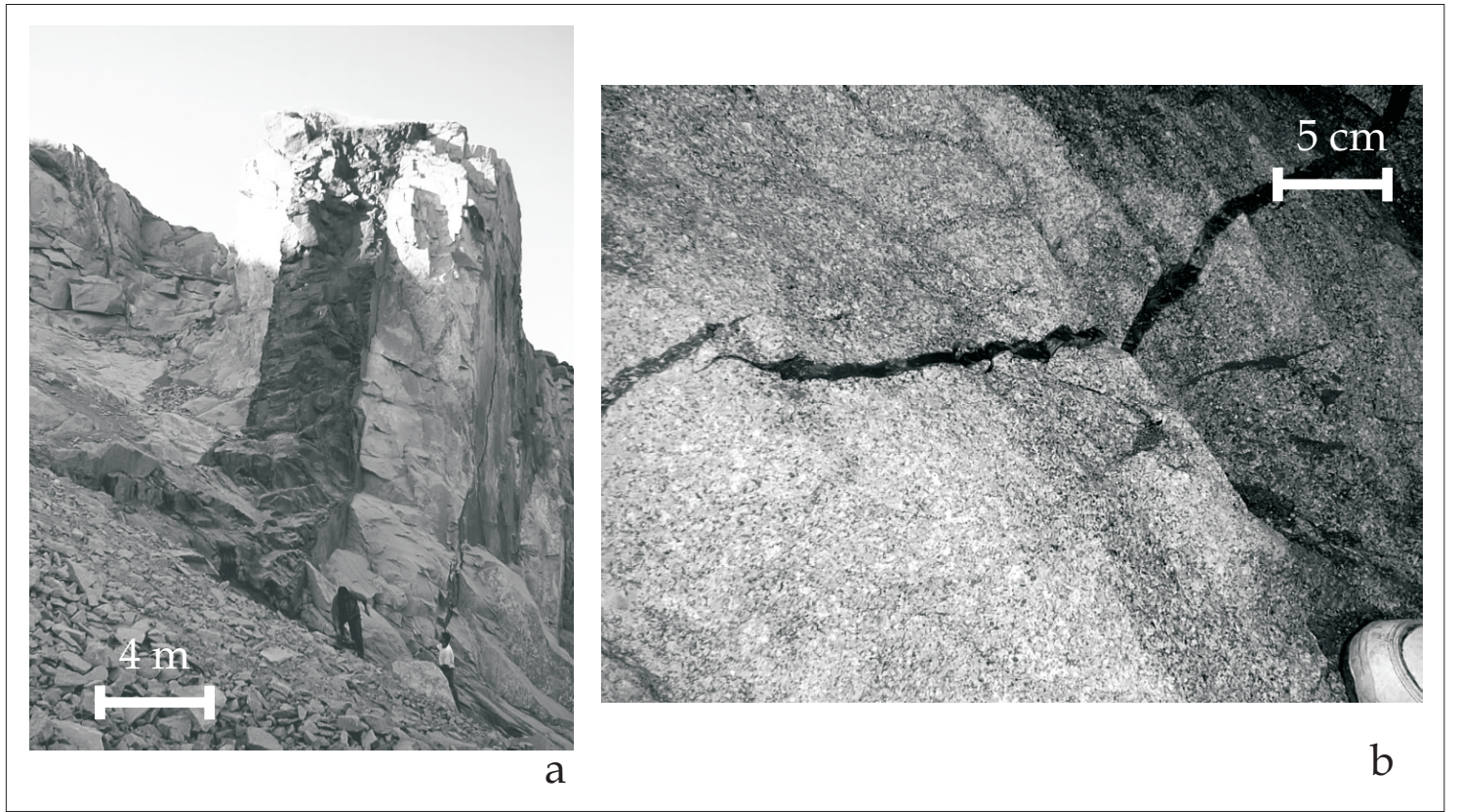


Figure 3

Figure 4

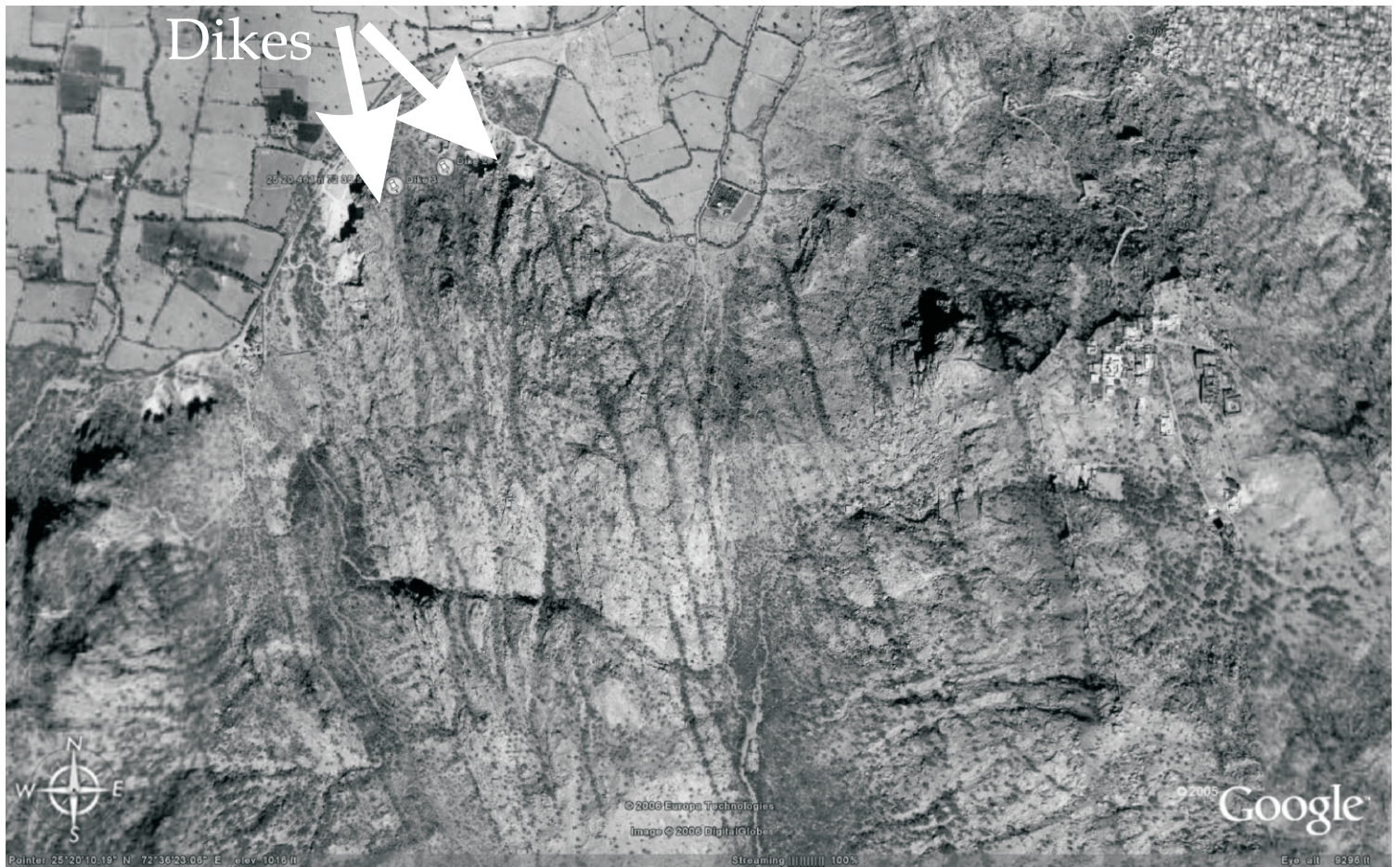


Figure 4

Figure 5



Figure 5

Figure 6

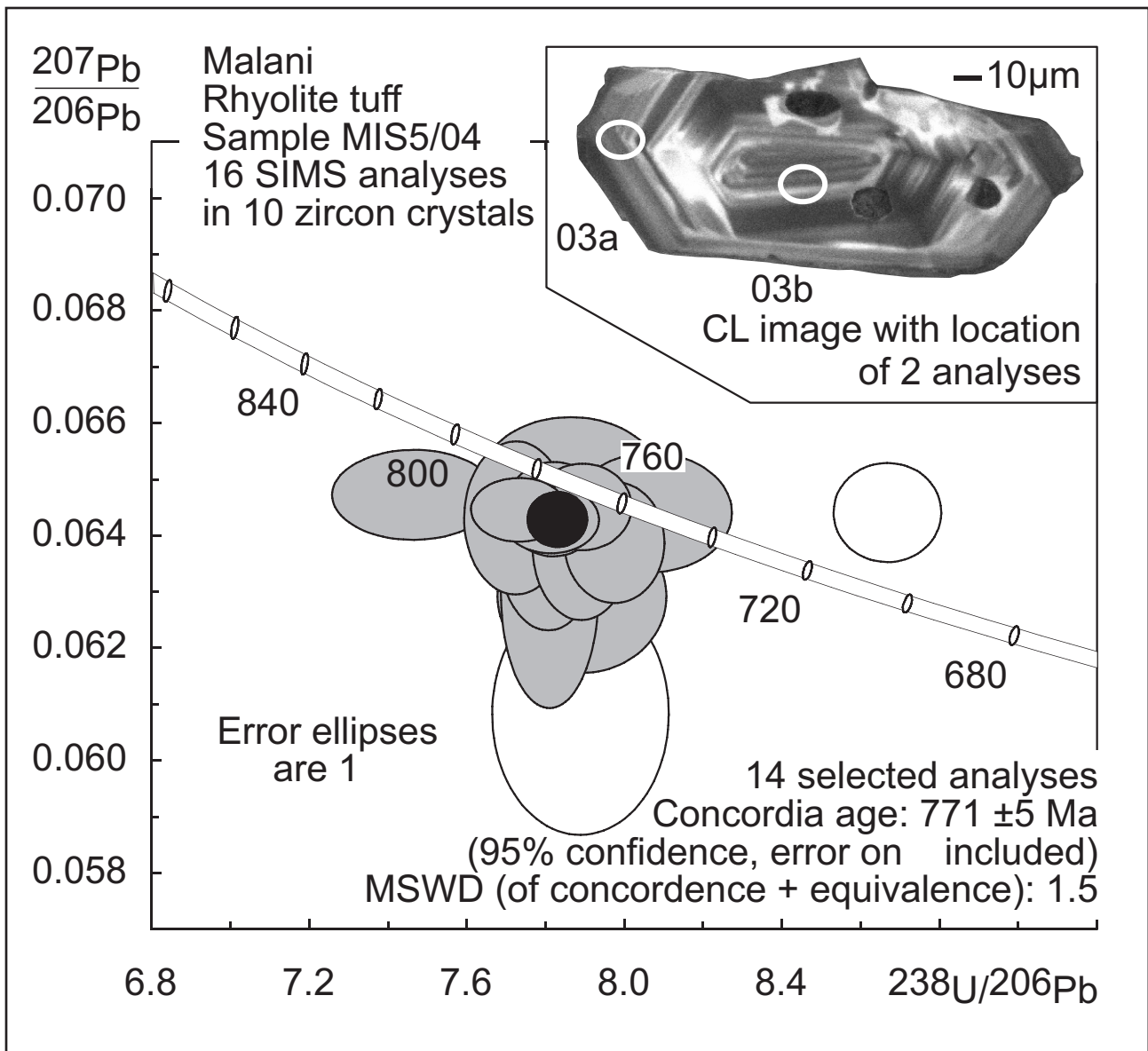


Figure 6

Figure 7

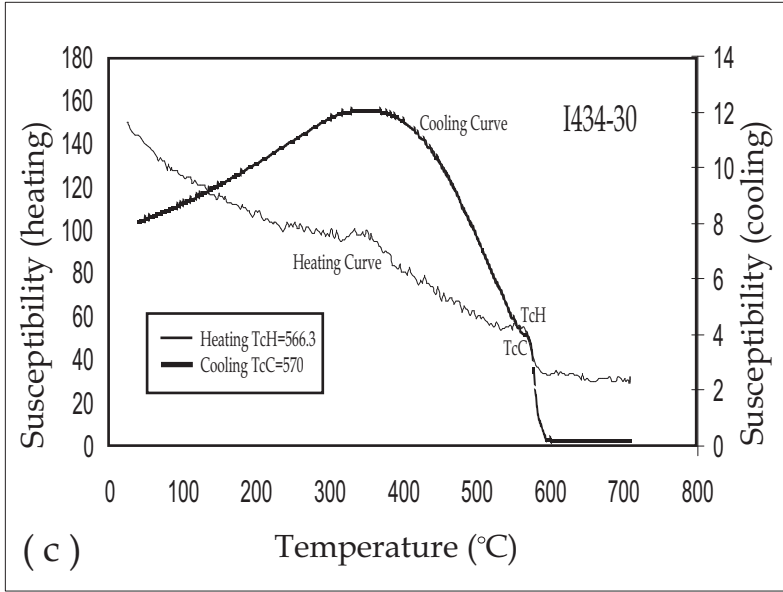
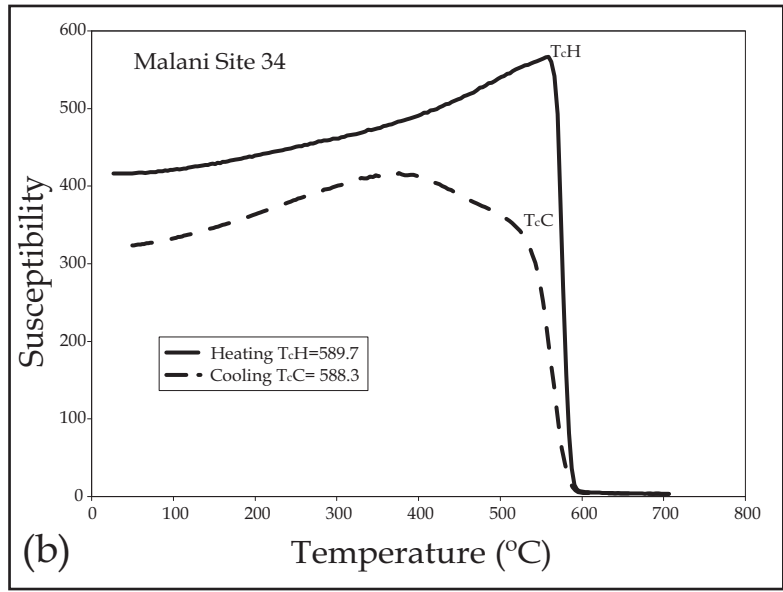
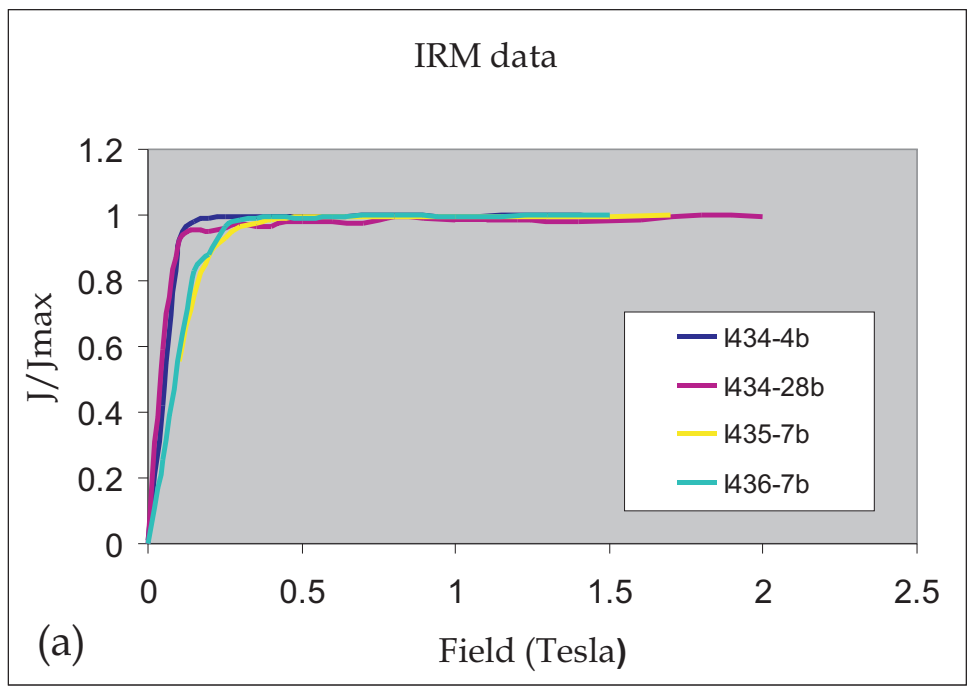
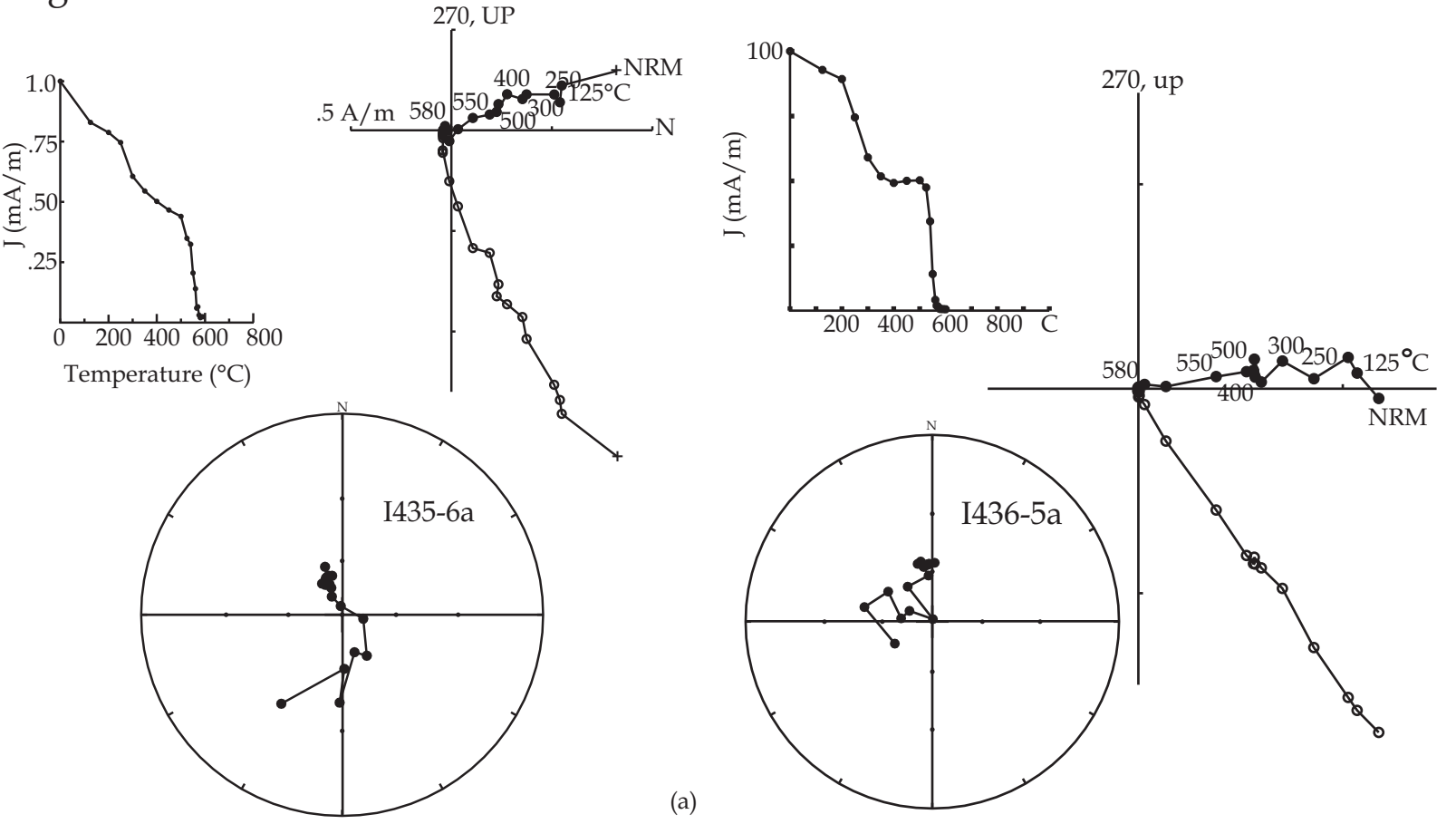
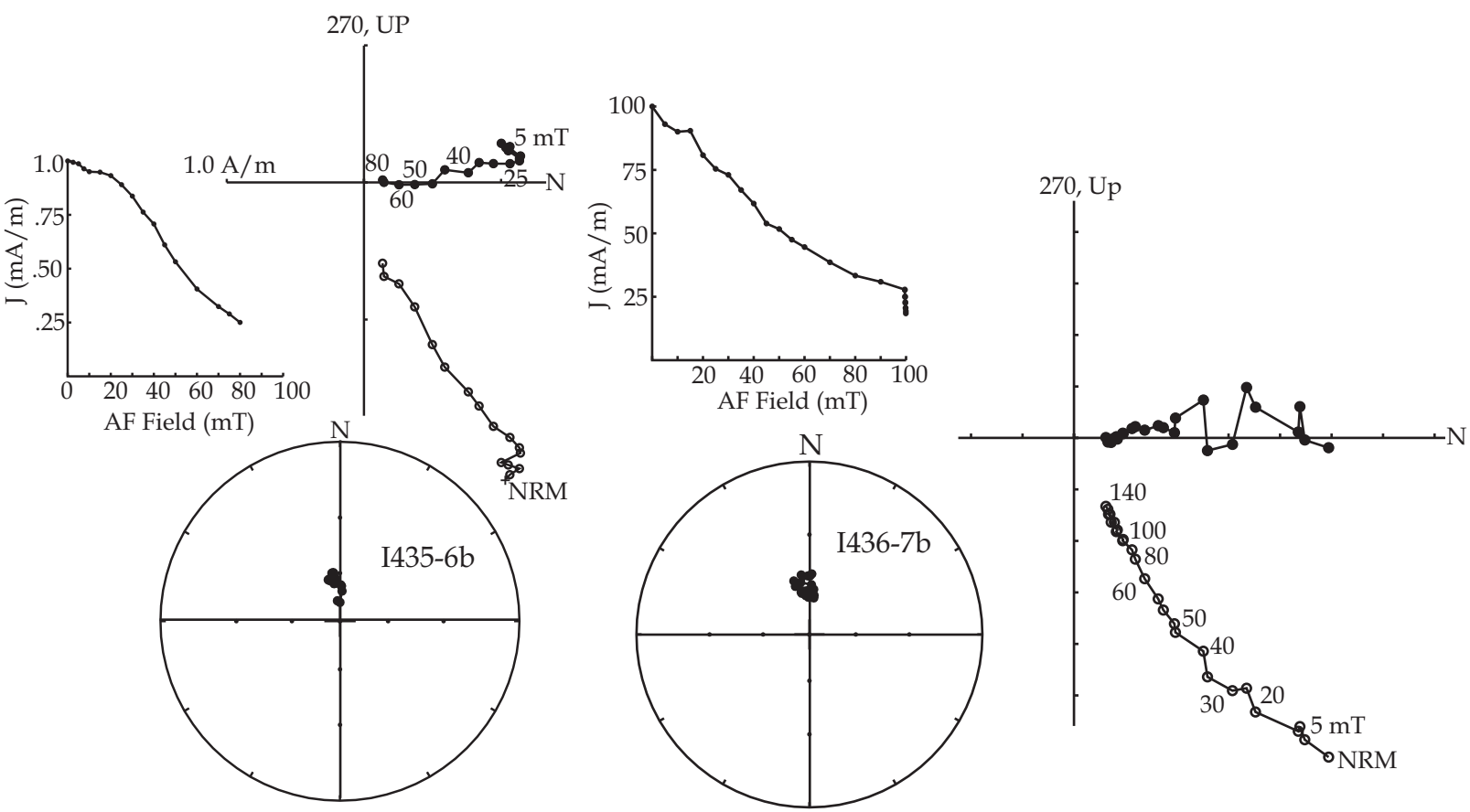


Figure 7

**Figure 8**



(a)



(b)

Figure 9

Figure 9

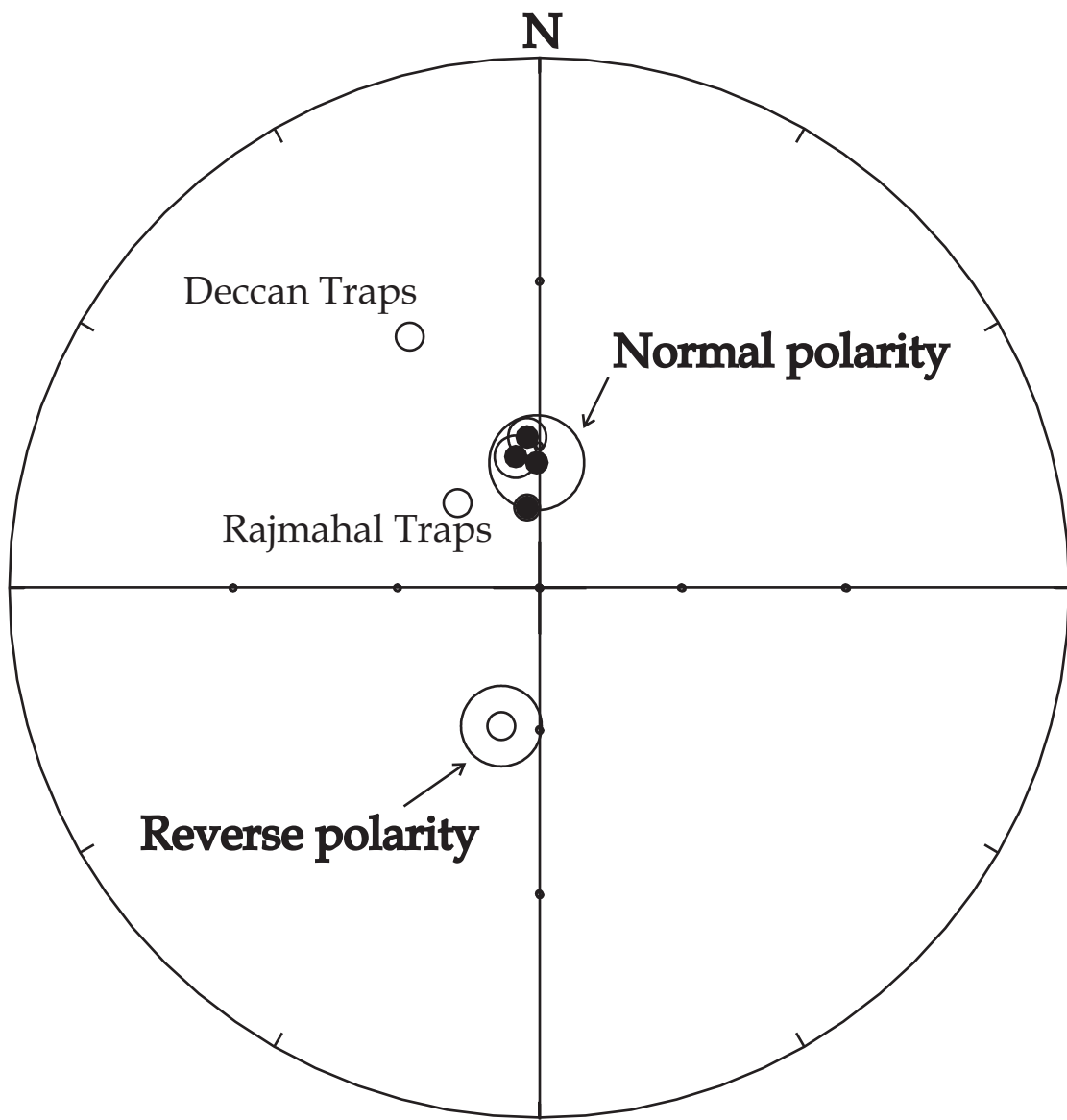
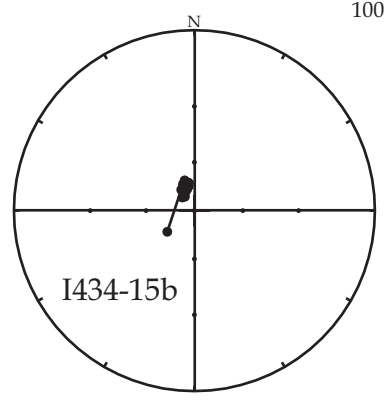
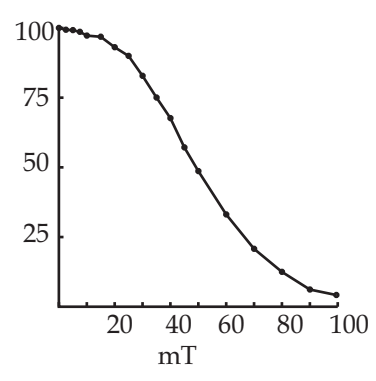
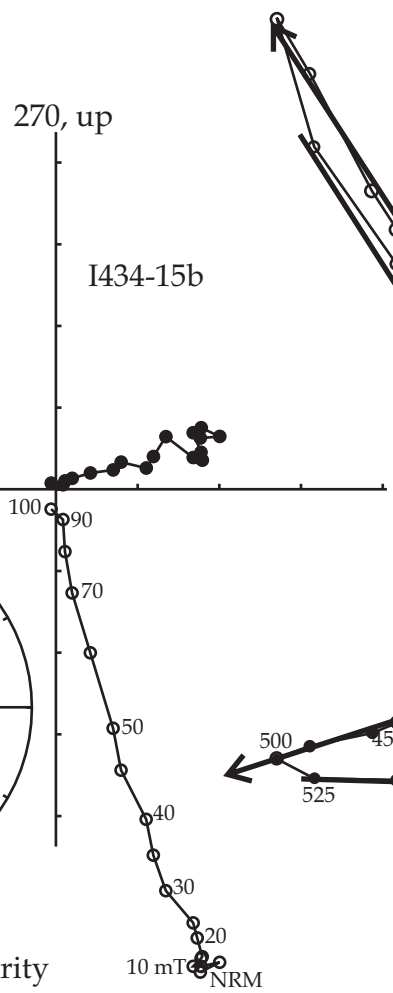


Figure 10

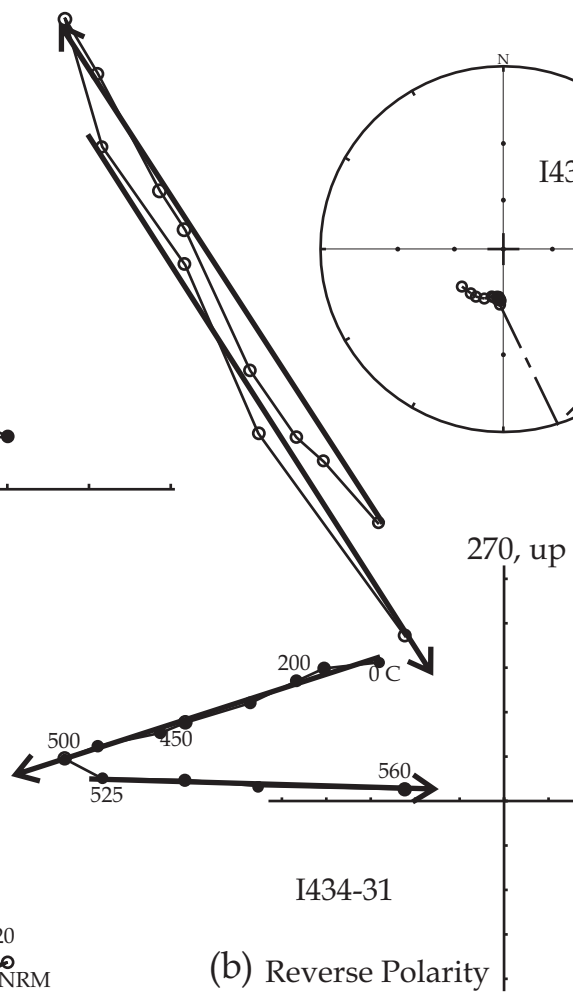
Figure 10



(a) Normal Polarity



10 mT NRM



(b) Reverse Polarity

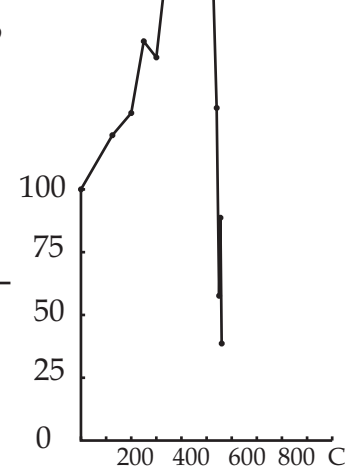
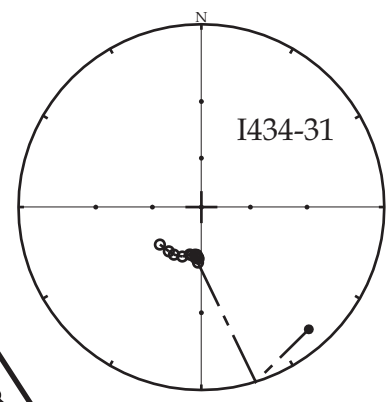


Figure 11

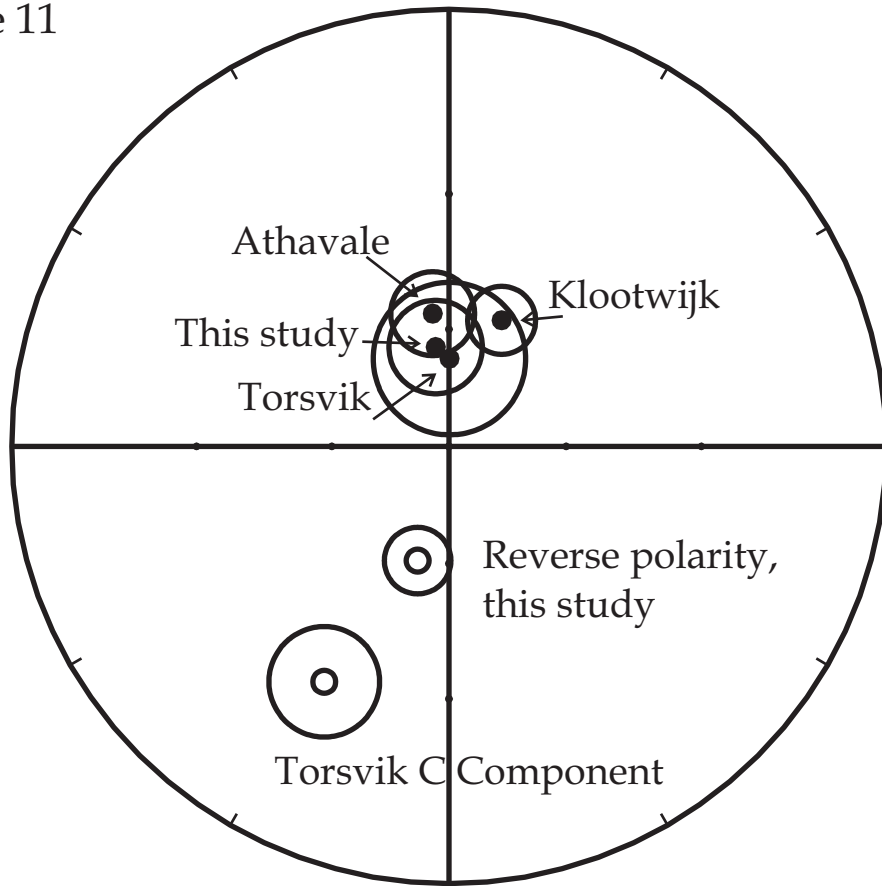
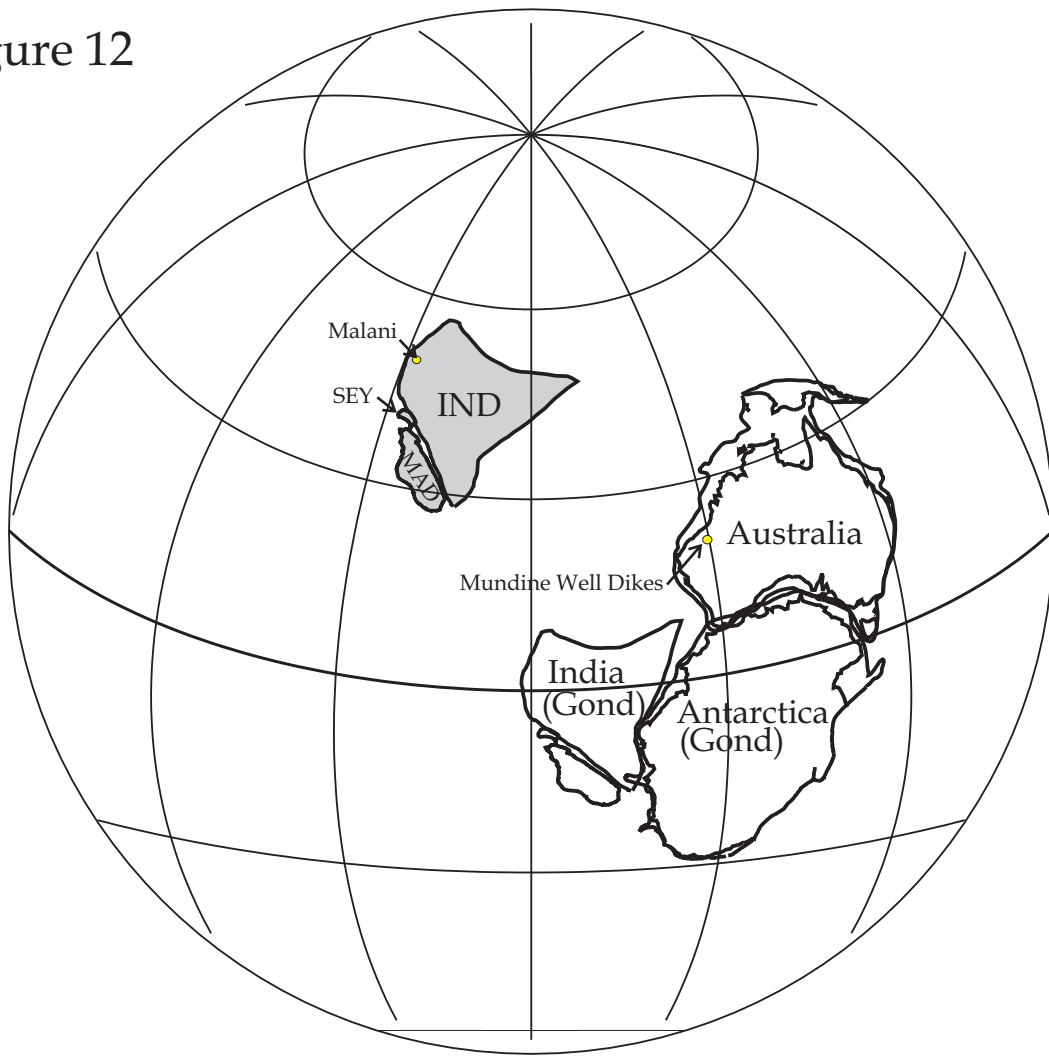


Figure 12



**Table 1**

Table 1: Summary of Paleomagnetic Poles

Pole Name	Age (Ma)	Pole latitude	Pole longitude	A95 or dp/dm <sup>a</sup>	dec <sup>b</sup>	inc <sup>b</sup>	$\alpha_{95}$ <sup>c</sup>	$\kappa$ <sup>d</sup>	Reference
<b>India</b>									
Malani, aplite dike	750	74.6 N	49.8 E	16.2	352.5	60	16.2	18.6	Rao et al., 2003
Malani, rhyolite	745±10	80.5 N	43.5 E	8/11.5°	354.5	53.5	8		Klootwijk, 1975
Malani, felsic volcanics	751±3, 771±2	74.5 N	71.2 E	7.4/9.7°	359.5	60.4	6.4	29.9	Torsvik et al., 2001
Malani, rhyolite	740	78.0 N	45.0 E	11.0/15.0°	353	56	10		Athavale et al., 1963
Malani, mafic dikes, felsic volcanics*	771±5*	69.0 N	83.2 E	8.8/10.9°	349.8	64.1	11.5	116.44	this study, *site 3 of Torsvik et al, 2001a
<b>Seychelles</b>									
Mahe dikes <sup>IND</sup>	750.2±2.5	79.8 N	78.6 E	9.9/14.9°	1.4	49.7	11.2		Torsvik et al., 2001
<b>Australia</b>									
Mundine Well dikes <sup>IND</sup>	755	41.47 N	130.92 E	4.1/4.1°	14.8	31.1	5		Wingate and Giddings, 2000

a:  $A_{95}$ = cone of 95% confidence about the mean pole; dp/dm cone of 95% confidence about the paleomagnetic pole in the co-latitude direction (dp) and at a right angle to the co-latitude

b: dec/inc= mean declination/ inclination

c:  $\alpha_{95}$ = circle of 95% confidence about the mean

d:  $\kappa$ = kappa precision parameter

le direction (dm).

Table 2: Summary of Geochronologic Results

Site	Study	Method	Age (Ma)
<b><i>Malani</i></b>			
rhyolites	Crawford and Compston (1970)	Rb/Sr (recalc with new constant)	730±10
rhyolites	Klootwijk (1975)	Rb/Sr	745±10
felsic volcanics	Rathore et al. (1996)	Rb/Sr isochron	779±10
ultrapotassic rhyolites	Rathore et al. (1999)	Rb/Sr isochron	681±20
Jalore granites	Rathore et al. (1999)	Rb/Sr isochron	727±8
peralkaline volcanics	Rathore et al. (1999)	Rb/Sr isochron	693±8
rhyolite	this study, site 3 of Torsvik et al., 2001a	U/Pb	771±5

Table 3

Table 3: SIMS zircon U–Pb data on rhyolite tuff from Malani igneous suite.

ID	U (ppm)	Th (ppm)	Pb (ppm)	$^{206}\text{Pb}$ <sup>a</sup>	$^{207}\text{Pb}$	$\pm\sigma$ (%)	$^{207}\text{Pb}$	$\pm\sigma$ (%)	$^{206}\text{Pb}$	$\pm\sigma$ (%)	R <sup>b</sup>	$^{206}\text{Pb}$ <sup>c</sup>	$\pm\sigma$	$^{206}\text{Pb}$ <sup>d</sup>	$\pm\sigma$	Disc. <sup>e</sup> 2 $\sigma$ lim. (%)
				$^{204}\text{Pb}$	$^{206}\text{Pb}$		$^{235}\text{U}$		$^{238}\text{U}$			$^{238}\text{U}$		$^{238}\text{U}$		
MIS5/04: rhyolite tuff <sup>f</sup>																
n1808-01a <sup>g</sup>	222	120	31	10257	0.06439	0.9	1.024	1.4	0.1154	1.0	0.75	704	7	703	7	
n1808-03a	414	202	64	17681	0.06449	0.8	1.127	1.3	0.1267	1.0	0.79	769	8	770	8	
n1808-03b	400	175	62	22494	0.06444	0.6	1.149	1.2	0.1294	1.0	0.87	784	8	785	8	
n1808-04a	85	63	14	5821	0.06372	1.5	1.126	1.8	0.1281	1.0	0.57	777	8	779	8	
n1808-05a	183	106	29	28736	0.06445	0.9	1.137	1.4	0.1279	1.0	0.77	776	8	777	8	
n1808-05b	196	149	33	6602	0.06430	1.4	1.148	1.8	0.1295	1.1	0.62	785	8	786	9	
n1808-05c	55	31	9	3629	0.06296	2.2	1.112	2.4	0.1281	1.0	0.43	777	8	779	8	
n1808-06a	149	113	24	6027	0.06385	1.1	1.104	1.5	0.1254	1.1	0.68	762	8	762	8	
n1808-06b	134	99	22	8903	0.06380	1.4	1.115	1.7	0.1268	1.0	0.60	769	8	771	8	
n1808-07a	401	316	67	13951	0.06426	0.6	1.134	1.2	0.1280	1.0	0.86	777	8	777	8	
n1816-01a	143	101	23	6033	0.06493	1.2	1.139	2.3	0.1272	1.9	0.85	772	14	772	15	
n1816-01b	197	154	32	14111	0.06377	1.0	1.119	2.2	0.1273	2.0	0.89	772	14	773	15	
n1816-02a <sup>g</sup>	46	24	7	3182	0.06076	2.4	1.062	3.0	0.1268	1.9	0.62	770	14	774	14	0.5
n1816-03a	88	57	14	13350	0.06288	1.4	1.099	2.3	0.1268	1.8	0.78	769	13	771	13	
n1816-03b	200	164	35	15016	0.06472	0.8	1.196	2.0	0.1340	1.8	0.91	811	14	812	14	
n1816-06a	138	54	20	10092	0.06440	1.1	1.101	2.0	0.1240	1.7	0.84	754	12	754	12	

a: Measured  $^{206}\text{Pb}/^{204}\text{Pb}$  ratio

b: R, correlation coefficient of errors in isotopic ratios

c:  $^{204}\text{Pb}$  corrected aged:  $^{207}\text{Pb}$  corrected agee: age discordance at the closest approach of 2  $\sigma$  error ellipse to concordia

f: coordinates of the sample: 26°17.963'-72°58.357'

g: analysis not selected for calculation of concordia age

Table 4: Paleomagnetic results

Site name	Lat/Long	n/N <sup>a</sup>	Declination	Inclination	Kappa ( $\kappa$ ) <sup>b</sup>	$\alpha_{95}$ <sup>c</sup>	VGP latitude <sup>d</sup>	VGP longitude <sup>d</sup>	dp, dm <sup>e</sup>
I434 (normal)	25° 20.517'N, 72° 36.084'E	23/27	351.4	72.6	129.55	2.7	56.9N	64.3E	4.3, 4.8
I434 (reverse)	25° 20.517'N, 72° 36.084'E	3/3	195.3	-59.7	234.79	8.1	70.2N	108.8E	9.2, 12.2
I435	25° 20.483'N, 72° 36.057'E	6/8	349.8	61.8	244.78	4.3	70.5N	49.8E	5.1, 6.7
I436	25° 20.461'N, 72° 36.992'E	9/9	355.4	58.2	256.88	3.8	75.9N	57.7E	4.1, 5.6
Combined mean		4 dikes	349.8	64.1	116.44	11.5			

a: n= samples used; N= samples collected

b:  $\kappa$ = kappa precision parameter

c:  $\alpha_{95}$ = circle of 95% confidence about the mean

d: VGP latitude/longitude = virtual geomagnetic pole

e: dp,dm= cone of confidence along site latitude (dp) and orthogonal to site latitude (dm)